Journal of chemical & engineering data

Article

pubs.acs.org/jced

Melting Points of Potential Liquid Organic Hydrogen Carrier Systems Consisting of *N*-Alkylcarbazoles

Katharina Stark,[†] Philipp Keil,[†] Sebastian Schug,[†] Karsten Müller,[*,†] Peter Wasserscheid,[‡] and Wolfgang Arlt[†]

[†]Institute of Separation Science and Technology, and [‡]Institute of Chemical Reaction Engineering, Friedrich-Alexander-Universität Erlangen-Nürnberg, Egerlandstraße 3, 91058 Erlangen, Germany

Supporting Information

ABSTRACT: Liquid organic hydrogen carriers (LOHCs) represent an attractive concept for storing hydrogen by the hydrogenation of usually aromatic compounds. One of the best investigated LOHCs is *N*-ethylcarbazole because of its favorable thermodynamic properties. However, its high melting point of 343.1 K could be a major drawback particularly in mobile applications. Therefore, it is desired to decrease the melting point of *N*-ethylcarbazole without significantly changing favorable properties such as the storage density or the reaction behavior of the carrier compound. To investigate the solid−liquid behavior during hydrogenation, the melting points of pure *N*-ethylcarbazole derivatives with increasing degree of hydrogenation as well as the liquidus line of the binary mixture of *N*-ethylcarbazole and *N*-ethyl-dodecahydro-carbazole were measured. Because of their structural and chemical resemblance binary mixtures consisting of different alkylcarbazole combinations were analyzed regarding their potential for a melting point depression. By the appropriate combination of *N*-alkylcarbazoles, it is possible to achieve a considerable melting point decrease to 297.1 K.

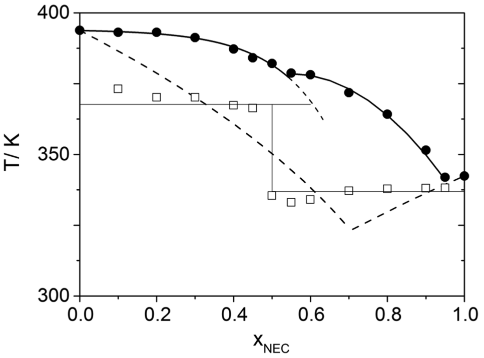

1. INTRODUCTION

Liquid organic hydrogen carriers (LOHCs) are novel media for the storage and transport of energy in the form of hydrogen. The concept is based on a reversible catalytic hydrogenation reaction of organic compounds that offer a high hydrogen storage capacity. Among others, *N*-ethylcarbazole (0H-NEC) is a very promising candidate which was first proposed as a potential LOHC by Pez et al. in 2004.[1] Since then *N*-ethylcarbazole has become one of the most intensively investigated LOHCs.[2−11] *N*-ethylcarbazole stores 12 atoms of hydrogen in the form of its fully hydrogenated derivative *N*-ethyl-dodecahydro-carbazole.[12] This results in a high storage density of 5.8 wt %. Moreover also several other properties of *N*-ethylcarbazole are beneficial for its use as LOHC, such as nontoxicity, low vapor pressure, low dehydrogenation temperatures due to favorable thermodynamics, and a comparatively high rate of reaction for the dehydrogenation of the hydrogenated form.

Many authors consider the high melting point of *N*-ethylcarbazole of 343.1 K[13] as the major drawback for its use as LOHC in stationary and particularly mobile applications.[14−16] To ensure that the compound does not solidify during storage or transport, it would be necessary to heat all process equipment which is in contact with LOHC constantly to a temperature above 343.1 K. This results in an additional energy demand as well as higher capital expenditure.[9]

Therefore, it was the objective of this work to examine different options for decreasing the melting point of *N*-ethylcarbazole to melting points at least below ambient temperature.

Pure *N*-ethylcarbazole is considered to be the highest melting compound in the LOHC system. During the hydrogenation of *N*-ethylcarbazole a multinary mixture containing different partly hydrogenated derivatives is formed (refer to Figure 1 for the

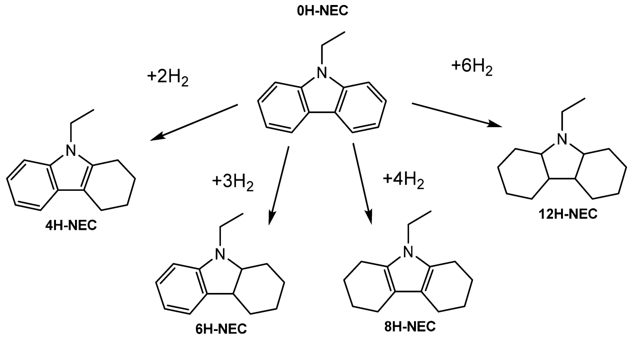

Figure 1. Partly and fully hydrogenated derivatives of *N*-ethylcarbazole.[4−6]

Received: August 9, 2015
Accepted: March 3, 2016
Published: March 17, 2016

DOI: 10.1021/acs.jced.5b00679
J. Chem. Eng. Data 2016, 61, 1441−1448

Table 1. Investigated *N*-Alkylcarbazoles Purified by Means of Crystallization and Analyzed by GC−MS

chemical name	abbreviation	source	CAS	final mole fraction purity
carbazole	C	Merck KGaA	86-74-8	0.995
tetrahydrocarbazole	4H-C	Alfa Aesar	942-01-8	0.995
N-methylcarbazole	NMC	Sigma-Aldrich	1484-12-4	0.995
N-ethylcarbazole	(0H)-NEC	Sigma-Aldrich	86-28-2	0.999
N-propylcarbazole	NPC	Akos Cons. & Solutions GmbH	1484-10-2	0.995
N-isopropylcarbazole	NiPC	Apollo Scientific	1484-09-9	0.999
N-butylcarbazole	NBC	Akos Cons. & Solutions GmbH	1484-08-8	0.995

Table 2. Investigated Partly and Fully Hydrogenated Derivatives of *N*-Ethylcarbazole and Carbazole Purified by Means of Fractional Batch Distillation and Analyzed by GC−MS. Source of Components: Institute of Reaction Engineering, University of Erlangen-Nuremberg

Chemical Name	Abbreviation	Structure	Final mole fraction purity
N-ethyl-tetrahydro-carbazole	4H-NEC	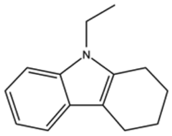	0.999
N-ethyl-octahydro-carbazole	8H-NEC	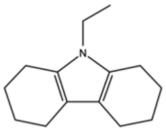	0.998
N-ethyl-dodecahydro-carbazole	12H-NEC	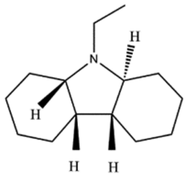	0.999
Tetrahydro-carbazole	4H-C	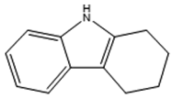	0.995
Dodecahydro-carbazole (diastereomeric mixture)	12H-C	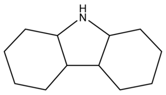	0.990

most important intermediates). In the following those derivatives are abbreviated as *x*H-NEC, where *x* denotes the number of hydrogen atoms reversibly bound to the *N*-ethylcarbazole molecule (or just *x*H-C, if the dehydrogenated form is carbazole). It was reported that the resulting multinary mixture of different partly hydrogenated derivatives leads to a melting point depression.[15]

Thus, incomplete dehydrogenation might be an option for a melting point decrease. However, to the best of our knowledge no quantitative data on the melting points of the partly hydrogenated *N*-ethylcarbazoles *N*-ethyl-tetrahydro-carbazole (4H-NEC), *N*-ethyl-hexahydro-carbazole (6H-NEC), and *N*-ethyl-octahydro-carbazole (8H-NEC) are available in the literature. To close this gap the melting points of pure intermediates were measured in this work.

The solid−liquid behavior of the multinary hydrogenation mixtures is very complex due to the number of involved components, and the resulting complex crystallization behavior. For simplification reasons, the liquidus curve of the binary system *N*-ethylcarbazole and its perhydrogenated derivative *N*-ethyl-dodecahydro-carbazole was measured in the first place.

Another approach for decreasing the melting point is based on the substitution of *N*-ethylcarbazole by another alkylcarbazole derivative with a lower melting point. In that way comparable hydrogenation reaction properties can be achieved.[17] The melting point of the homologous series of *N*-alkylcarbazoles strongly depends on the length of the alkyl chain.[6] It is known from literature that the melting point decreases from the nonalkylated carbazole (T_m = 518.3 K[18]) to *N*-propylcarbazole (T_m = 322.2 K[19]). *N*-Isopropycarbazole with a branched alkyl chain shows a considerably higher melting point (T_m = 395.2 K[20]) than its linear isomer. By a further increase of the chain length the melting point starts to increase again which is indicated by the melting point of *N*-butylcarbazole (T_m = 331.0 K[19]). Because the availability of melting point data especially for *N*-propylcarbazole and *N*-butylcarbazole in the literature is rather poor, additional property data are reported in this work.

Combining different *N*-alkylcarbazoles might be also an attractive option for achieving a melting point depression in the case of eutectic solid−liquid phase behavior. Owing to the lack of literature data, melting enthalpies of pure *N*-alkylcarbazoles as well as their binary solid–liquid phase behavior have been determined in this work.

2. EXPERIMENTAL SECTION

2.1. Materials. Table 1 shows the *N*-alkylcarbazoles investigated in this contribution. The purity was confirmed by gas chromatography–mass spectroscopy (GC–MS), and if required, the purchased substances were further purified by recrystallization from cyclohexane or acetone to obtain a final purity of ≥99.5% (GC–MS).

Table 2 shows the partly and fully hydrogenated derivatives of *N*-etylcarbazole and carbazole investigated in this paper. A reaction mixture containing different hydrogenation products was prepared by hydrogenation of *N*-ethylcarbazole (0H-NEC) at 150 °C and 40 bar hydrogen pressure in a stainless steel autoclave equipped with a gas entry stirrer. Ru (5 wt %) on alumina support was used as catalyst. The reaction product was filtered through a frit at the bottom of the autoclave.[13]

The different intermediates as well as the fully hydrogenated 12H-NEC were separated from the reaction mixture by fractional batch distillation and analyzed by means of NMR and GC–MS. 0H-NEC, 4H-NEC, 6H-NEC, 8H-NEC and at least three diastereomers of 12H-NEC were identified.[21] 12H-NEC was separated from the mixture by distillation with a high purity of >99.9%. On the basis of the NMR measurements it is assumed that the asymmetric dodecahydro-*N*-ethylcarbazole (see Table 2) was obtained, which has already been described by Eblagon[4−6] to be the most stable one. The purity of the partly hydrogenated substances 4H-NEC and 8H-NEC which were also separated from the reaction mixture by distillation was determined to be >99.8% (GC–MS). Because of 6H-NEC being formed as a stable intermediate during (de)-hydrogenation to a far lesser extent than 4H-NEC and 8H-NEC, it could not be separated in a sufficient amount and purity. A diastereomeric mixture of 12H-C was prepared by catalytic hydrogenation of 4H-C analogous to the procedure described above. 12H-C was recrystallized from a mixture of acetone and toluene (50/50 wt %) to obtain a final purity >99.0%. The diasteromeric mixture was not further separated. The partly and fully hydrogenated products were stored at temperatures below 253 K under argon atmosphere to prevent degradation.

2.2. DSC Measurements. *Sample Preparation. N-Alkylcarbazoles.* For the pure component measurements, 3–8 mg of sample in solid or liquid state was sealed in an aluminum crucible. At least three crucibles were prepared for each substance.

The different binary mixtures of two *N*-alkylcarbazoles were prepared by weighing at least 0.1 g of each solid component into a glass vial depending on the desired molar ratio. Subsequently the substances were melted by heating them and then mixed by shaking the vial until a homogeneous solution was obtained. After that the samples were stored in a refrigerator at 253 K, ensuring a quick solidification of the mixture. Briefly before measurement the solid samples were ground at room temperature to homogenize the mixture. Samples containing carbazole (nonalkylated) were not melted before grinding up to avoid degradation because of the high melting point of carbazole (T_m = 518 K).[18] Consequently they were not stored in a refrigerator. For each DSC measurement 3–8 mg of sample was sealed in an aluminum crucible. Liquid samples were mixed by shaking the vial until a homogeneous solution was obtained and filled as a liquid into aluminum crucibles.

Reaction Intermediates. Crucibles containing *N*-ethyl-octahydro-carbazole or tetrahydro-carbazole which were sealed under air atmosphere did not show reproducible experimental results. The enthalpy of fusion decreased with repeated measurements. Additionally an exothermic effect was observed directly after the solid–liquid transition. Therefore, it was assumed that the samples showed degradation during DSC analysis because of a reaction of *N*-ethyl-octahydro-carbazole or tetrahydro-carbazole, respectively, with the oxygen present in air in the crucibles.

Crucibles containing *N*-ethyl-octahydro-carbazole or tetrahydro-carbazole, respectively, which were sealed in a glovebox (oxygen, ≤20 ppm; water, ≤0.5 ppm) to ensure the absence of oxygen, did not show this exothermic effect but gave reproducible results.

Samples containing *N*-ethyl-tetrahydro-carbazole had to be stored in a refrigerator for several days until they were fully crystallized because of the very slow crystallization kinetics of the compound.

Experimental Procedure. The DSC measurements were performed using a Maia 200 differential scanning calorimeter (DSC) from Netzsch. The temperature range and program of the measurements was adapted depending on the melting points of the components.

The DSC was calibrated with respect to enthalpy of fusion and melting temperature using a Netzsch certified calibration set containing the six compounds indium, adamantane, tin, bismuth, zinc, and cesium chloride at very high purity 99.9% to 99.999% with melting point temperatures in the range of 218.7 K to 749.2 K and enthalpies of fusions in the range of 17.2 J/g to 107.5 J/g. Additionally the certified calibration compound biphenyl with a purity of 99.5%, a melting point of 342.1 K, and enthalpy of fusion of −120.4 J/g, was used for calibration to incorporate an organic compound with structural similarity to the *N*-alkylcarbazoles. After calibration, the melting point of indium was determined with a standard uncertainty of 0.1 K, and the standard uncertainty of enthalpy of fusion was determined to be 0.1 J/g.

The measurements have been evaluated using the software Proteus 5.2 (Netzsch). For pure substances the onset point of the peak represents the start of the solid–liquid phase change which indicates the melting point. If the binary mixture demonstrates eutectic behavior, two peaks are formed. The onset of the first peak indicates the eutectic temperature while the peak point of the second peak represents the melting temperature owing to the dissolution of the last solid. In case of eutectic composition of the sample, only one peak is formed.[22]

2.3. Static Measurements. Static measurements have been performed for the determination of the liquidus curve for the binary mixture of *N*-ethylcarbazole and *N*-ethyl-dodecahydro-carbazole. DSC measurements were found to be not suitable for mixtures of these two substances because of the slow crystallization kinetics. Therefore, both substances were put into a 100 mL stirred glass vessel in defined shares and heated to the desired temperature so that both phases, solid and liquid, coexisted. The total mass during the experiments was approximately 50–100 g of substance depending on the desired concentration. Then both substances were stirred intensively at defined, constant temperatures controlled by a LAUDA PROLINE RP845 thermostat until equilibrium was reached. After that the stirrer was switched off and a liquid sample was withdrawn using a syringe. The temperature of the vessel was measured with a calibrated Pt-100 placed in the middle of the liquid phase during sample taking. To minimize the amount of solid particles in the withdrawn sample, a PTFE syringe filter with a pore size of 5.0 μm (Rotilabo) was used. The concentration of the samples was determined quantitatively by GC (FID)-analysis. Sampling for each temperature was performed at least two times.

3. RESULTS AND DISCUSSION

3.1. Pure Component Data. *3.1.1. Melting Point Behavior during (De)hydrogenation.* Table 3 shows the pure component data for the *N*-ethylcarbazole and carbazole derivatives with different degrees of hydrogenation which were obtained by DSC measurements and a comparison with literature values.

Table 3. Melting Points $T_{m,0i}$ and Enthalpies of Fusion $\Delta_{fus}h_{0i}$ (at $T_{m,0i}$) of Different *N*-Alkylcarbazoles and Their (Partly) Hydrogenated Derivatives at Pressure p = 0.1 MPa[a]

substance	$T_{m,0i}$/K	$\Delta_{fus}h_{0i}$/kJ mol^{-1}	source
carbazole (C)	517.1 ± 0.2	27.70 ± 0.31	this work
	518.33 ± 0.01	27.08 ± 0.48	18
	521.2	27.2	23
	518.7	26.9	24
N-methylcarbazole (NMC)	361.0 ± 0.3	16.43 ± 0.22	this work
	362.5	17.15	25
N-ethylcarbazole (NEC)	342.4 ± 0.1	16.55 ± 0.17	this work
	343.1	15.10 ± 0.40	13
N-propylcarbazole (NPC)	320.4 ± 0.2	19.57 ± 0.13	this work
	322.2 ± 4.0		19
N-iso-propylcarbazole (NiPC)	393.9 ± 0.3	18.26 ± 0.33	this work
	395.2	17.73	20
N-butylcarbazole (NBC)	330.6 ± 0.1	22.80 ± 0.16	this work
	331.0 ± 4.0		19
N-ethyl-tetrahydro-carbazole	282.4 ± 0.1	12.41 ± 0.04	this work
N-ethyl-octahydro-carbazole	316.0 ± 0.1	20.58 ± 0.19	this work
N-ethyl-dodecahydro-carbazole	188.6 (T_G)		this work
tetrahydro-carbazole	391.3 ± 0.1	17.85 ± 0.06	this work
dodecahydro-carbazole	349.5 ± 0.4	22.91 ± 0.72	this work

[a] The uncertainties of the melting point and enthalpy of fusion correspond to expanded uncertainties of the mean (0.95 confidence level). Standard uncertainties u are $u(T)$ = 0.1 K, $u(p)$ = 5 kPa.

The melting points of the *N*-ethylcarbazole derivatives do not show a clear trend with increasing degree of hydrogenation, as the melting point of 8H-NEC is higher than that of 4H-NEC. However, both components show a lower melting point than 0H-NEC.

For 12H-NEC only a glass transition was observed during DSC measurements. The substance did not crystallize even after storing it in a glass vial at temperatures less than 245 K for more than a year. Subsequently also no enthalpy of fusion was obtained.

The change in melting point in dependence of the degree of hydrogenation was compared to carbazole derivatives which constitute the main impurity in *N*-ethylcarbazole reaction mixtures. By the addition of four hydrogen atoms the melting point of carbazole with 517.1 K drops to 391.3 K for 4H-C. By the addition of 12 hydrogen atoms the melting point further decreases to 349.5 K. The higher experimental error of 12H-C in comparison to the other substances can be explained by the fact that 12H-C is not a pure compound but a diastereomeric mixture.

3.1.2. Variation of the Alkyl Chain. The melting points of the *N*-alkylcarbazoles with linear alkyl chain decrease with increasing chain length up to *N*-propylcarbazole (see Table 3). The higher melting point of *N*-butylcarbazole as compared to *N*-propylcarbazole indicates that the melting point increases with a further increase of the chain length. *N*-Isopropylcarbazole with a branched alkyl chain shows a higher melting point compared to the linear N-propylated derivative, which might be because of its rather symmetric structure. The measured melting temperatures are in good agreement with literature data.

The enthalpy of fusion of carbazole (27.70 kJ/mol) is higher than for *N*-methylcarbazole (16.43 kJ/mol) or *N*-ethylcarbazole (16.55 kJ/mol). This effect propably occurs because of the larger influence of the N atom inducing a slight polarity in carbazole, which is weaker in *N*-methylcarbazole and *N*-ethylcarbazole. With a further increase of the length of the side chain, the enthalpy of fusion increases again but still does not reach the value of carbazole. The measured enthalpies of fusion are in good agreement with literature data.

3.2. Binary Mixtures. *3.2.1. Modeling of the Phase Behavior.* Binary solid–liquid equilibria (SLE) were modeled using eq 1.

$$\ln\frac{f_i^{0,L}}{f_i^{0,S}} = \ln\left(\frac{x_i^L\cdot\gamma_i^L}{x_i^S\cdot\gamma_i^S}\right) = -\frac{\Delta_{fus}h_{0i}}{RT}\left[1-\frac{T}{T_{m,0i}}\right] - \frac{\Delta c_p}{R}\left[1-\frac{T_{m,0i}}{T}-\ln\frac{T_{m,0i}}{T}\right] \quad (1)$$

Equation 1 describes the ratio of standard fugacity f_i^0 of the liquid phase L and solid phase S with the measurable thermodynamic variables of the pure component enthalpy of fusion $\Delta_{fus}h_{0i}$, the melting temperature $T^*_{m,0i}$ and the difference in heat capacities Δc_p of solid and liquid state. Further x_i is the molar fraction, R is the ideal gas constant, and γ_i^φ is the activity coefficient in the respective phase φ.

Equation 1 can be simplified using the following assumptions: (i) ideal eutectic behavior with crystallization of pure solid phase i: x_i^S = 1; γ_i^S = 1; (ii) difference in heat capacities between solid and liquid phase is small: $\Delta c_p \approx 0$. With these assumptions eq 2 is obtained:

$$\ln(x_i^L\cdot\gamma_i^L) = -\frac{\Delta_{fus}h_{0i}}{RT}\left[1-\frac{T}{T_{m,0i}}\right] \quad (2)$$

In the case that the liquid phase behaves as an ideal mixture, γ_i^L = 1 holds and eq 3 is obtained which represents the most simplified expression for describing the solubility of a component i.

$$\ln(x_i^L) = -\frac{\Delta_{fus}h_i}{RT}\left[1-\frac{T}{T_{m,i}}\right] \quad (3)$$

Only the pure component properties, enthalpy of fusion and melting point of the involved components, are required for modeling the liquidus line of an ideal eutectic mixture.[25,26]

3.2.2. Binary Mixtures of N-Ethylcarbazole Derivatives with Different Degree of Hydrogenation. During hydrogenation the melting point of the reaction mixture decreases.[15] The solid−liquid behavior of these multinary hydrogenation mixtures is very complex. To get a basic understanding of the phase behavior, the liquidus lines for the binary mixture *N*-ethylcarbazole (NEC) and *N*-ethyl-dodecahydro-carbazole (12H-NEC) was measured (see Figure 2).

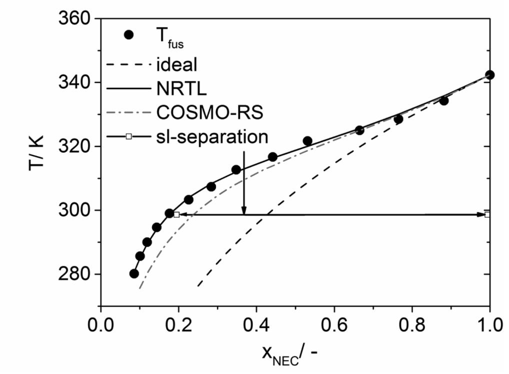

Figure 2. Solid−liquid phase diagram of the system *N*-ethylcarbazole (NEC) and *N*-ethyl-dodecahydro-carbazole (12H-NEC). Experimental data (symbols), calculated liquidus lines assuming ideal phase behavior (ideal), and liquidus lines calculated for real phase behavior with activity coefficients obtained by fitting the experimental data to the NRTL-model (NRTL) and with activity coefficients predicted by COSMO-RS (COSMO-RS).

As described previously, the solid−liquid equilibrium of the system was measured by using a static method. With increasing molar fraction of *N*-ethyl-dodecahydro-carbazole the melting point decreases. At 298.6 K, a solid−liquid phase separation experiment was performed to determine the composition of the formed solid phase (indicated by arrows in Figure 2). An aliquot of the well-mixed suspension was extracted with a syringe. The two phases were separated in a filter centrifuge and the crystals were washed twice with cyclohexane to remove adhering liquid phase. The concentration of *N*-ethyl-dodecahydro-carbazole in the solid phase after washing was determined to be 0.6% while the concentration of the coexisting liquid phase lies on the liquidus line. Therefore, it can be stated that rather pure *N*-ethylcarbazole is crystallized as solid phase from the binary mixture.

The deviation between the experimental data $x_{i,\mathrm{exp}}$ and the calculated points on the ideal liquidus line $x_{i,\mathrm{calc}}$ was evaluated quantitatively with the standard deviation σ and the relative error δ (see eqs 4 and 5).

$$\sigma = \sqrt{\frac{\sum_{i=1}^{n} (x_{i,\mathrm{exp}} - x_{i,\mathrm{calc}})^2}{(n-1)}} \tag{4}$$

$$\delta = \frac{\sum_{i=1}^{n} \left| \frac{x_{i,\mathrm{exp}} - x_{i,\mathrm{calc}}}{x_{i,\mathrm{exp}}} \right|}{n} \tag{5}$$

With increasing amount of 12H-NEC the measured values show an increasing positive deviation from the ideal predicted liquidus line which is the reason for the resulting values of σ = 0.2 and δ = 98.6% being quite high.

Owing to the differences between experimental and ideal calculated values, activity coefficients greater than 1 result. The thus obtained activity coefficients were fitted using the well-known NRTL-model[26] (eqs 6−11). The parameters are summarized in Table 4.

$$\ln \gamma_i^{\mathrm{L}} = \frac{\sum_j x_j \tau_{ji} G_{ji}}{\sum_k x_k G_{ki}} + \sum_k \frac{x_j G_{ij}}{\sum_k x_k G_{kj}} \left(\tau_{ij} - \frac{\sum_m x_m \tau_{mj} G_{mj}}{\sum_k x_k G_{kj}} \right) \tag{6}$$

$$G_{ij} = \exp(-\alpha_{ij}\tau_{ij}) \tag{7}$$

$$\tau_{ij} = a_{ij} + \frac{b_{ij}}{T} \tag{8}$$

$$\alpha_{ij} = c_{ij} + d_{ij}(T - 273.15\ \mathrm{K}) \tag{9}$$

$$\tau_{ii} = 0 \tag{10}$$

$$G_{ii} = 1 \tag{11}$$

Table 4. NRTL Regression Parameters for the Binary Mixture 0H-NEC−12H-NEC at Pressure p = 0.1 MPa

NRTL T/K	i = 0H-NEC, j = 12H-NEC
a_{ij}	0
a_{ji}	0
b_{ij}	−3274.28415
b_{ji}	4100.5343
c_{ij}	9.87×10^{-03}
d_{ij}	0

For an a priori prediction of liquid phase activity coefficients γ_i^{L} in order to determine the solid−liquid phase behavior, COSMO-RS (COSMOthermX, C21_0111) was used.[27] The COSMO-RS calculations predict activity coefficients greater than 1. The trend of the liquidus line was predicted correctly, resulting in lower values for σ (0.05) and δ (22.9%). However, the absolute values of the activity coefficients are still underestimated.

3.2.3. Binary Mixtures of Different N-Alkylcarbazoles.

Figure 3 shows the binary SLE of six different *N*-alkylcarbazole combinations.

The eutectic temperatures for the six binary solid−liquid equilibria are summarized in Table 5. The binary mixtures NEC−C, NEC−NMC, and NEC−NPC show only a slight positive deviation of the ideal calculated liquidus curve. The minor differences between ideal calculated and experimental obtained values are within the uncertainty of measurement.

The binary SLE of NPC−NBC also demonstrates eutectic behavior with a further solid−solid transition at T = 284 K for compositions with x_{NEC} > 0.5, that is, on the *N*-ethylcarbazole-rich side of the phase diagram. A similar phase behavior has been observed in a recent study on the solid−liquid equilibria of triolein with fatty acids.[28]

The system NEC and NiPC shows a strong deviation from the ideal calculated liquidus curve. Up to a concentration of x_{NEC} = 0.5, a phase transition at a constant temperature of T = 367.7 K is found, while for higher concentrations, a phase transition at a constant temperature of T = 336.9 K is found. The data of the liquidus line indicate a discontinuity in the region around x_{NEC} = 0.55 which can be interpreted to be a peritectic point. On the basis of the results obtained in this work, a peritectic phase behavior with incongruent melting behavior is proposed. In region (I) the melt and solid *N*-isopropyl-carbazole are in equilibrium. In region (II), the melt

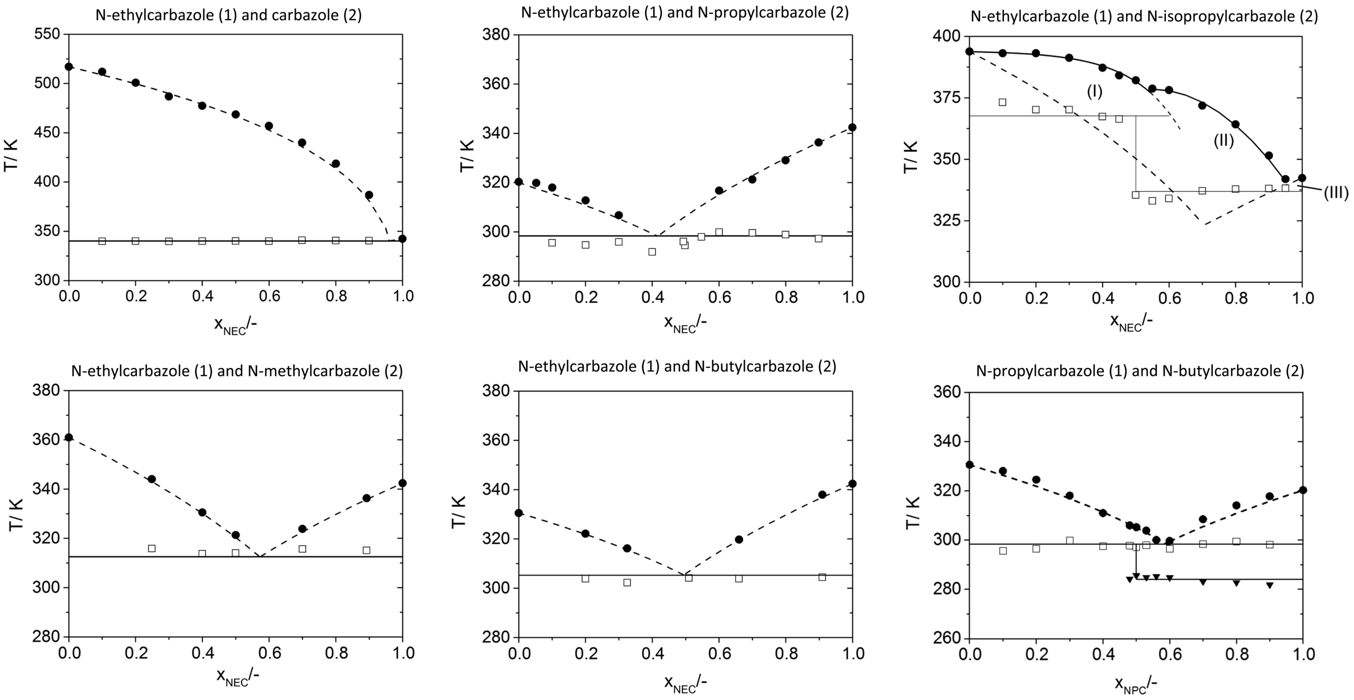

Figure 3. Binary phase diagrams of six combinations of different *N*-alkylcarbazoles: □, T_{eu} = eutectic temperature; ●, T_{fus} = temperature of fusion; ▼, T_{tr} = temperature of transition; ---, ideal calculated liquidus lines (eq 3).

Table 5. Ideal Calculated Eutectic Temperature $T_{eu,id}$ and Eutectic Temperature $T_{eu,exp}$ of the Binary SLEs at the Eutectic Concentration $x_{NEC,eu}$ (for Abbreviations of the Compounds See Table 3)

mixture	$x_{NEC,eu}$	$T_{eu,id}$/K	$T_{eu,exp}$/K	σ/K	δ/%	hydrogen storage capacity at $x_{NEC,eu}$/wt %
NEC−C	0.96	340.3	340.2	3.9	0.76	5.8
NEC−NMC	0.57	312.5	314.9	1.0	0.25	6.0
NEC−NPC	0.42	298.2	297.1	1.7	0.44	5.6
NEC−NiPC	0.72	323.1	336.9	30.7	7.10	5.7
NEC−NBC	0.49	305.5	303.8	0.71	0.16	5.4
NPC−NBC	0.59	298.7	297.7	1.8	0.43	5.3

[a] Standard uncertainties u are $u(T_m)$ = 1 K, $u(T_{eu})$ = 2 K, $u(x)$ = 0.001, $u(p)$ = 5 kPa.

and a solid 1:1-mixture of the components coexist, and in region (III) the melt and solid *N*-ethylcarbazole coexist. The eutectic point is around x_{NEC} = 0.95; however, this work focused on the investigation of the liquidus curve and hence the solid phenomena were not further investigated.

The deviation between the experimental data and the calculated points on the ideal calculated liquidus line $T_{i,exp} - T_{i,calc}$ was evaluated quantitatively with the standard deviation σ and the relative error δ.

$$\sigma = \sqrt{\frac{\sum_{i=1}^{n} (T_{i,exp} - T_{i,calc})^2}{(n-1)}} \tag{12}$$

$$\delta = \frac{\sum_{i=1}^{n} \left| \frac{T_{i,exp} - T_{i,calc}}{T_{i,exp}} \right|}{n} \tag{13}$$

Comparing the eutectic temperatures of the analyzed mixtures it can be concluded that the lowest melting temperatures in binary systems are obtained using the mixtures NEC−NPC, NEC−NBC, and NPC−NBC which have eutectic points around room temperature. Therefore, a significant melting point decrease can be achieved compared to pure *N*-ethylcarbazole.

By enlarging the chain length of the alkyl group the gravimetric hydrogen storage capacity decreases. However, using a NEC−NPC mixture at eutectic composition, the hydrogen capacity is still 5.6 wt % while the melting point is reduced to 298 K compared to 5.8 wt % and 342 K for pure NEC.

Multinary mixtures, derived by mixing more than two *N*-alkylcarbazoles, might offer an even lower melting point. Because of the low eutectic temperatures measured for the binary systems NEC−NPC, NEC−NBC, and NPC−NBC, it seems reasonable to investigate the solid−liquid phase behavior of a ternary mixture consisting of these three substances. Therefore, the ternary eutectic temperature was calculated using the simplified Schroeder-van-Laar equation for ideal eutectic systems assuming that like the binary subsystems, also the ternary system shows ideal liquid phase behavior (see Figure 4).

A ternary eutectic temperature of T = 285.7 K was calculated for the mixture NEC−NPC−NBC while still offering a storage capacity of 5.5 wt % which is 95% of the capacity of pure NEC. The ideal calculations show that multinary mixtures containing three or more different alkylcarbazoles offer a simple solution with a very attractive potential for further decreasing the

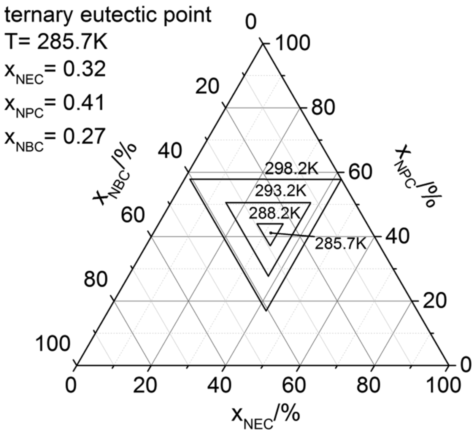

Figure 4. Ternary SLE diagram of the system NEC−NPC−NBC calculated assuming ideal liquid phase behavior.

melting point of a LOHC system to temperatures below ambient.

Because of the very slow crystallization behavior of this ternary mixture, DSC measurements were not performed in this work, but should be the subject of further investigations. The slow crystallization kinetics of mixtures consisting of carbazole derivatives may mislead experimentalists to believe that the mixtures have melting points far below room temperature. Therefore, one should keep in mind that liquid carbazole mixtures are able to crystallize even after more than a month storage time.

4. SUMMARY

The high melting point of *N*-ethylcarbazole is often mentioned as the main drawback for its use as a liquid organic hydrogen carrier;[14−16] therefore, different approaches for achieving a melting point depression preferably to temperatures below ambient were investigated.

Incomplete dehydrogenation might be an efficient measure for a sufficient melting point depression. The melting points of *N*-ethylcarbazole derivatives with different degrees of hydrogenation decrease in the following order: 0H-NEC, 8H-NEC, 4H-NEC, 12H-NEC. Because of a partly hydrogenated LOHC system being a multinary mixture, the solid−liquid behavior is very complex. The melting point decreases with increasing amount of 12H-NEC. However, 80% of 12H-NEC are necessary to keep a binary mixture of NEC−12H-NEC liquid at room temperature. This would drastically reduce the effective hydrogen storage density. Hence, on the basis of the current knowledge an incomplete dehydrogenation does not seem to be a reasonable solution particularly considering the loss in hydrogen storage capacity.

An alternative approach is to change the length of the alkyl chain in order to find an alkylcarbazole having a significantly lower melting point than *N*-ethylcarbazole. The melting point decreases with increasing chain length from carbazole to *N*-propylcarbazole and tends to increase again from *N*-butylcarbazole on. The branched *N*-isopropyl-carbazole has a comparatively higher melting point in comparison to its linear isomer *N*-propylcarbazole. Substituting *N*-ethylcarbazole by *N*-propylcarbazole, the melting point of the fully dehydrogenated LOHC can be reduced from 342.4 to 320.4 K. However, this is accompanied by a slight reduction in hydrogen storage density. Moreover, none of the investigated derivatives fulfill the objective of a melting point below ambient temperature.[29]

Therefore, binary mixtures of *N*-alkylcarbazoles were investigated regarding their melting point behavior at different concentrations, preferably in the case of eutectic phase behavior. Ideal eutectic behavior was observed for the binary mixtures NEC−C, NEC−NMC, NEC−NPC, and NEC−NBC. For the binary mixture NEC−NiPC a nonideal phase behavior was observed. On the basis of the experimental results, the system is proposed to be peritectic. This work shows that binary mixtures of *N*-alkylcarbazoles offer an attractive option to achieve a significant melting point decrease while keeping a high storage capacity. The mixture NEC−NPC at eutectic composition offers a hydrogen storage capacity of 5.6 wt % and is liquid down to T_{eu} = 297.1 K.

Multinary mixtures might be an option for a further melting point decrease. The prediction of the ternary eutectic point for the mixture NEC−NPC−NBC indicates a melting point of 285.7 K while still reaching a storage capacity of 5.5 wt %.

Mixtures of different *N*-alkylcarbazoles hence are a very attractive option to provide a LOHC system which combines a high effective hydrogen storage density and melting points which are over the whole degree of hydrogenation significantly below ambient temperature. Consequently the focus of further investigations should lie on the reaction and property behavior of *N*-alkylcarbazole mixtures during hydrogenation and dehydrogenation reaction in order to model the time-dependent occurring equilibria in the system as well as the whole LOHC-process and finally ensure a reliable process control. Besides the melting point future works should also investigate other important substance properties like the viscosity of these multicomponent mixtures.

■ ASSOCIATED CONTENT

Ⓢ Supporting Information

The Supporting Information is available free of charge on the ACS Publications website at DOI: 10.1021/acs.jced.5b00679.

Conditions of the DSC measurements (PDF)

■ AUTHOR INFORMATION

Corresponding Author

*E-mail: karsten.mueller@fau.de.

Notes

The authors declare no competing financial interest.

■ ACKNOWLEDGMENTS

The authors thank Prof. Dr. Axel König and Dr. Matthias Kick for helpful discussions and support of this work. We want to thank Roswitha Eckstein for assistance during the experimental work and Katharina Obesser, Michael Müller, and Marcus Koch from the group of Prof. Dr. Peter Wasserscheid for the synthesis of chemical species.

■ REFERENCES

(1) Pez, G. P.; Scott, A. R.; Cooper, A. C.; Cheng, H. Hydrogen storage by reversible hydrogenation of pi-conjugated substrates. EP Patent EP1475349A2, 2004.

(2) Pez, G. P.; Scott, A. R.; Cooper, A. C.; Cheng, H.; Wilhelm, F. C.; Abdourazak, A. H. Hydrogen storage by reversible hydrogenation of pi-conjugated substrates. U.S. Patent US7351395B1, 2008.

(3) Pez, G. P.; Scott, A. R.; Cooper, A. C.; Cheng, H. Hydrogen storage by reversible hydrogenation of pi-conjugated substrates. U.S. Patent US20050002857A1, 2005.

(4) Eblagon, K. M.; Tam, K.; Yu, K. M. K.; Tsang, S. C. E. Comparative Study of Catalytic Hydrogenation of 9-Ethylcarbazole for Hydrogen Storage over Noble Metal Surfaces. *J. Phys. Chem. C* **2012**, *116*, 7421−7429.

(5) Eblagon, K. M.; Tam, K.; Tsang, S. C. E. Comparison of catalytic performance of supported ruthenium and rhodium for hydrogenation of 9-ethylcarbazole for hydrogen storage applications. *Energy Environ. Sci.* **2012**, *5*, 8621−8630.

(6) Eblagon, K. M.; Rentsch, D.; Friedrichs, O.; Remhof, A.; Zuettel, A.; Ramirez-Cuesta, A. J.; Tsang, S. C. Hydrogenation of 9-ethylcarbazole as a prototype of a liquid hydrogen carrier. *Int. J. Hydrogen Energy* **2010**, *35*, 11609−11621.

(7) Sotoodeh, F.; Smith, K. J. Structure sensitivity of dodecahydro-*N*-ethylcarbazole dehydrogenation over Pd catalysts. *J. Catal.* **2011**, *279*, 36−47.

(8) Sotoodeh, F.; Huber, B. J. M.; Smith, K. J. Dehydrogenation kinetics and catalysis of organic heteroaromatics for hydrogen storage. *Int. J. Hydrogen Energy* **2012**, *37*, 2715−2722.

(9) Teichmann, D.; Stark, K.; Muller, K.; Zottl, G.; Wasserscheid, P.; Arlt, W. Energy storage in residential and commercial buildings via Liquid Organic Hydrogen Carriers (LOHC). *Energy Environ. Sci.* **2012**, *5*, 9044−9054.

(10) Teichmann, D.; Arlt, W.; Wasserscheid, P.; Freymann, R. A future energy supply based on Liquid Organic Hydrogen Carriers (LOHC). *Energy Environ. Sci.* **2011**, *4*, 2767−2773.

(11) Teichmann, D.; Arlt, W.; Wasserscheid, P. Liquid Organic Hydrogen Carriers as an efficient vector for the transport and storage of renewable energy. *Int. J. Hydrogen Energy* **2012**, *37*, 18118−18132.

(12) Mehranfar, A.; Izadyar, M.; Esmaeili, A. A. Erratum to "Hydrogen storage by N-ethylcarbazol as a new liquid organic hydrogen carrier: A DFT study on the mechanism. *Int. J. Hydrogen Energy* **2015**, *40*, 7420−7421.

(13) Verevkin, S. P.; Emel'yanenko, V. N.; Pimerzin, A. A.; Vishnevskaya, E. E. Thermodynamic Analysis of Strain in the Five-Membered Oxygen and Nitrogen Heterocyclic Compounds. *J. Phys. Chem. A* **2011**, *115*, 1992−2004.

(14) Brueckner, N.; Obesser, K.; Boesmann, A.; Teichmann, D.; Arlt, W.; Dungs, J.; Wasserscheid, P. Evaluation of industrially applied heat-transfer fluids as liquid organic hydrogen carrier systems. *ChemSusChem* **2014**, *7*, 229−235.

(15) Sotoodeh, F.; Smith, K. J. An overview of the kinetics and catalysis of hydrogen storage on organic liquids. *Can. J. Chem. Eng.* **2013**, *91*, 1477−1490.

(16) Klebanoff, L. *Hydrogen Storage Technology: Materials and Applications*; CRC Press: Boca Raton, 2013.

(17) Yang, M.; Dong, Y.; Fei, S.; Pan, Q.; Ni, G.; Han, C.; Ke, H.; Fang, Q.; Cheng, H. Hydrogenation of N-propylcarbazole over supported ruthenium as a new prototype of liquid organic hydrogen carriers (LOHC). *RSC Adv.* **2013**, *3*, 24877−24881.

(18) Sabbah, R.; Watik, L. E. New reference materials for the calibration (temperature and energy) of differential thermal analysers and scanning calorimeters. *J. Therm. Anal.* **1992**, *38*, 855−863.

(19) Lopatinskii, V. P.; Sirotkina, E. E.; Sukhoroslova, M. M. N-Alkylcarbazoles. *Metody Poluch. Khim. Reakt. Prep.* **1964**, *11*, 69−72.

(20) Krajewska-Cizio, A. Phase diagrams in the binary systems of N-isopropylcarbazole with 2,4,7-trinitrofluoren-9-one and carbazole. *Thermochim. Acta* **1990**, *158*, 317−325.

(21) Stark, K.; Westerholt, A.; Wasserscheid, P.; Arlt, W. Trennung komplexer Mischungen von partiell hydrierten organischen Verbindungen und ihrer Isomere durch Destillation. *Chem. Ing. Tech.* **2012**, *84*, 1269−1269.

(22) Höhne, G.; Hemminger, W.; Flammersheim, H. J. *Differential Scanning Calorimetry*; Springer-Verlag: Berlin Heidelberg, 2003.

(23) Radomska, M.; Radomski, R. Calorimetric studies of binary systems of 1,3,5-trinitrobenzene with naphthalene, anthracene and carbazole. I. Phase transitions and heat capacities of the pure components and charge-transfer complexes. *Thermochim. Acta* **1980**, *40*, 405−414.

(24) Lisicki, Z.; Jamróz, M. E. (Solid + liquid) equilibria in (polynuclear aromatic + tertiary amide) systems. *J. Chem. Thermodyn.* **2000**, *32*, 1335−1353.

(25) Domalski, E. S.; Hearing, E. D. Heat Capacities and Entropies of Organic Compounds in the Condensed Phase. Volume III. *J. Phys. Chem. Ref. Data* **1996**, *25*, 1−525.

(26) Renon, H.; Prausnitz, J. M. Local compositions in thermodynamic excess functions for liquid mixtures. *AIChE J.* **1968**, *14*, 135−144.

(27) Klamt, A.; Schuurmann, G. COSMO: a new approach to dielectric screening in solvents with explicit expressions for the screening energy and its gradient. *J. Chem. Soc., Perkin Trans. 2* **1993**, 799−805.

(28) Maximo, G. J.; Costa, M. C.; Meirelles, A. J. A. Solid-liquid equilibrium of triolein with fatty alcohols. *Braz. J. Chem. Eng.* **2013**, *30*, 33−43.

(29) DOE. Targets for onboard hydrogen storage for light duty fuel cell vehicles. http://energy.gov/sites/prod/files/2014/03/f12/targets_onboard_hydro_storage.pdf (accessed 05.12.2014).